ELSEVIER

Journal of Computational and Applied Mathematics 102 (1999) 119–141

JOURNAL OF COMPUTATIONAL AND APPLIED MATHEMATICS

Voronoi diagram and medial axis algorithm for planar domains with curved boundaries I. Theoretical foundations

Rajesh Ramamurthy, Rida T. Farouki *

Department of Mechanical Engineering and Applied Mechanics, University of Michigan, Ann Arbor, MI 48109, USA

Received 18 December 1997; received in revised form 10 June 1998

Abstract

In this first installment of a two-part paper, the underlying theory for an algorithm that computes the Voronoi diagram and medial axis of a planar domain bounded by free-form (polynomial or rational) curve segments is presented. An incremental approach to computing the Voronoi diagram is used, wherein a single boundary segment is added to an existing boundary-segment set at each step. The introduction of each new segment entails modifying the Voronoi regions of the existing boundary segments, and constructing the Voronoi region of the new segment. We accomplish this by (i) computing the bisector of the new segment with each of the current boundary segments; (ii) updating the Voronoi regions of the current boundary segments by partitioning them with these bisectors; and (iii) constructing the Voronoi region of the new segment as a union of regions obtained from the partitioning in (ii). When all boundary segments are included, and their Voronoi regions have been constructed, the Voronoi diagram of the boundary is obtained as the union of the Voronoi polygons for each boundary segment. To construct the medial axis of a planar domain, we first compute the Voronoi diagram of its boundary. The medial axis is then obtained from the Voronoi diagram by (i) removing certain edges of the Voronoi diagram that do not belong to the medial axis, and (ii) adding certain edges that do belong to the medial axis but are absent from the Voronoi diagram; unambiguous characterizations for edges in both these categories are given. Details of algorithms based on this theory are deferred to the second installment of this two-part paper.

Keywords: Voronoi diagram; Medial axis; Bisectors; Distance functions; Bifurcation points

1. Introduction

The *Voronoi diagram* and *medial axis* of a closed bounded planar domain are fundamental geometrical entities associated with that domain. [1] The medial axis can be intuitively thought of as the locus of centers of maximum-radius circles (touching the boundary in at least two points) that may

* Corresponding author. E-mail: farouki@mae.engr.ucdavis.edu.

[1] For brevity we often abbreviate 'Voronoi diagram' and 'medial axis' to VD and MA.

0377-0427/99/$ – see front matter
PII: S0377-0427(98)00211-8

be inscribed within the domain. The Voronoi diagram of a domain bounded by N curve segments, on the other hand, specifies a partition of the plane into N regions (not necessarily disjoint) such that each point within a given region is at least as close to its associated boundary segment as to all other segments.[2]

Apart from their intrinsic geometrical interest, the computation of medial axes and Voronoi diagrams is a valuable preprocessing step in a variety of application contexts, such as finite element meshing [25, 42, 43]; font design [13]; tool path generation for NC machining [14, 26, 34]; surface fitting [23]; image compression [9]; pattern analysis and shape recognition [5, 6]; and the computation of equivalent resistance networks for VLSI circuits [30].

We shall focus here on Voronoi diagram and medial axis computations for planar domains with piecewise-analytic boundaries. There are, however, many interesting generalizations of this problem – e.g., computation of geodesic medial axes on free-form surfaces [28, 38] and multiscale medial axis algorithms for processing digitized gray-scale images [1, 20, 22, 32].

The Voronoi diagram and medial axis of a planar domain may be regarded as graphs, whose edges are portions of point/curve and curve/curve bisectors – i.e., loci that are equidistant from certain points or curve segments of the domain boundary. For domains with polygonal or piecewise-linear/circular boundaries, these bisectors are just conic arcs, and efficient algorithms have been developed that yield essentially *exact* Voronoi diagram and medial axis constructions [26, 27, 29, 35, 41, 45]. For domains with free-form (polynomial or rational) boundary curves, however, such constructions are more difficult since the curve/curve bisectors do not admit exact 'simple' representations [17]. Consequently, the latter problem has received less attention [2, 13, 15].

Our present aim is to employ earlier preparatory studies [16–19] of point/curve and curve/curve bisectors in developing an accurate and robust algorithm for constructing the Voronoi diagrams and medial axes of free-form planar domains. Note that this problem demands a specifically-formulated algorithm: making a piecewise-linear approximation of a free-form boundary and invoking a polygonal-domain algorithm, for example, generates results that are not even *qualitatively* (topologically) correct; see Section 2.2 below.

The guiding principles for the design of our Voronoi diagram/medial axis algorithm are: (i) to capture the exact (rational) parameterizations of those edges that admit them; (ii) to provide piecewise-rational approximations, that satisfy a prescribed geometrical tolerance, for the remaining edges; and (iii) to remain faithful, within the specified geometrical tolerance, to the true topology of the Voronoi diagram and medial axis.

Some highlights from earlier point/curve and curve/curve bisector studies that bear directly on the above principles are as follows:

- the bisector of a point and a polynomial or rational curve segment is generically rational [16] – it can be described exactly in, e.g., the customary rational Bézier form;
- the bisector of two polynomial or rational curves is not (in general) a rational locus, and hence must be approximated – but through use of point/curve bisectors as an intermediate tool, the generation of ordered sequences of point/tangent/curvature data on such loci can be reduced [17] to a family of univariate polynomial root-finding problems;

[2] Note that the medial axis depends only on the *geometry* of the boundary, whereas the Voronoi diagram depends also on its *segmentation*. Hence, the Voronoi diagram changes if a boundary segment is split in two, but the medial axis is unaffected (see also Section 7 below).

- error measures for geometric Hermite interpolants to such discrete data allow them, by means of adaptive subdivision, to approximate the true curve/curve bisector to any given tolerance, and singularities (tangent discontinuities) can be captured in an essentially exact manner [18];
- certain 'degenerate' forms of point/curve and curve/curve bisector, that require special treatment, arise generically in Voronoi diagram and medial axis computations [19]: for example, the bisector of two curves that share a common endpoint (which may be of mixed dimension – the union of a one-dimensional locus and a two-dimensional region);
- also, with free-form boundaries, a new type of bisector arises that was absent from the piecewise-linear/circular context: the *self-bisectors* of individual boundary segments – the treatment of all these degenerate bisector forms has been described in [19].

We encourage the reader to consult the cited references for complete details, and to acquire full preparation for the remainder of this paper.

Owing to the wealth of essential detail that the subject matter entails, we choose to present our results in a two-part paper. The present contribution concentrates on the theoretical foundations, and includes only a brief high-level algorithm description and simple illustrative examples. The companion paper [37] offers complete details of the algorithm and the numerical methods and data structures it employs, with more substantial computed examples. These papers parallel recent studies [12, 13] by Choi et al., although we adopt a quite different approach (based on explicit bisector computations).

Our plan for this paper is as follows. In Section 2 we summarize earlier work on Voronoi diagram and medial axis computations, highlight the inadequacy of polygonal approximations to curved boundaries, and review some basic facts concerning distance functions and bisector loci. Voronoi diagrams for planar domains with curved boundaries are defined in Section 3, and in Section 4 an algorithm for their construction is sketched, with emphasis on the key steps of Voronoi region partitioning and bifurcation point identification. The operation of this algorithm is illustrated in Section 5 by a simple example. Our attention turns to the medial axis in Section 6, and in Section 7 basic differences between Voronoi diagrams and medial axes are identified. In Section 8 we show how the algorithm can be extended to derive the medial axis from the Voronoi diagram, and the example of Section 5 is resumed to illustrate this. Finally, Section 9 offers some concluding remarks.

2. Preliminaries

2.1. Synopsis of earlier studies

Voronoi diagrams have been extensively discussed [36] in the computational geometry literature – mostly in the context of discrete point sets. Interest in developing Voronoi diagram/medial axis algorithms for continuous domains is somewhat more recent. A number of authors have contributed to elucidating their basic theoretical properties; see [3, 4, 7, 8, 10–12, 21, 24, 33, 40, 44].

The earliest Voronoi diagram/medial axis methods for planar domains were $O(n^2)$ algorithms that operated on digitized images of planar domains – see, e.g., [31]. Subsequently, more efficient algorithms based on computational geometry principles have been developed.

Preparata [35] proposed an $O(n \log n)$ incremental algorithm to construct the Voronoi diagram/medial axis of convex polygons. Lee [29] introduced the divide-and-conquer strategy in an algorithm

for non-convex polygons. An interesting feature of Lee's method is the status accorded to reflex vertices of the polygon as 'boundary elements' – on an equal footing with the polygon edges – which ensures that all the boundary elements will have mutually disjoint Voronoi regions (see Remark 3.2 below).

Natural extensions of the divide-and-conquer strategy allow for multiply-connected polygonal domains, as formulated by Srinivasan and Nackman [41], and for circular as well as linear segments of the domain boundary – see [26, 34, 45]. As noted in Section 1 above, these algorithms exhaust the range of boundary geometries that admit *exact* (i.e., rational) representations for their Voronoi diagram/medial axis edges.

Voronoi diagram and medial axis computations for domains with free-form boundaries are much more challenging, and have only recently begun to attract interest. Chou [15] describes a numerical method for tracing the medial axis from its 'terminal points' – i.e., convex corners or centers of curvature for vertices (points of extremum curvature) of the boundary, while Alt and Schwarzkopf [2] sketch an algorithm that presumes the availability of certain 'black-box' functions (bisector computations, etc.). However, these authors do not make as clear a distinction between the Voronoi diagram and the medial axis as we deem necessary here – see Sections 3, 6, and 7 below.

Finally, Choi et al. have presented mathematical foundations [12] and an approximation algorithm [13] for the medial axes of curvilinear domains. The latter is based on an ingenious domain decomposition scheme that identifies all the 'special' (i.e., terminal or bifurcation) points of the medial axis, and establishes their connectivity in a tree data structure. The 'simple' edges connecting these nodes are then amenable to approximation by interpolating point/tangent data. The algorithm can accommodate multiply-connected domains by invoking a preliminary step called *homology killing*.

Our own algorithm is the culmination of thorough investigations [16–19] of point/curve and curve/curve bisectors, that have served to establish their fundamental properties and practical algorithms for their computation. It is intended as a natural extension of the existing linear/circular-boundary algorithms, which proceed through successive refinement of Voronoi regions as the domain boundary segments are consecutively introduced. Through its more-sophisticated treatment of bisectors, the algorithm accommodates new phenomena that arise only in the case of curvilinear domains, and it captures exact (i.e., rational) representations for all edges that admit them.

2.2. Inadequacy of boundary approximations

As previously noted, robust and efficient algorithms to compute the Voronoi diagrams and medial axes of planar domains with polygonal (or piecewise-linear/circular) boundaries are available. In view of their relative simplicity, it might seem that an easy 'practical' approach to domains with free-form boundary curves is to first approximate the boundaries, within a prescribed tolerance, by polygonal or piecewise-linear/circular curves, and then invoke the currently available algorithms for such boundary curves.

However, this approach yields *qualitatively* (i.e., topologically) *incorrect* results, and the discrepancy between the 'true' Voronoi diagram/medial axis (for the exact boundary) and those for the approximate boundary grows as the tolerance on the latter is tightened by introducing further linear/circular approximating segments; see Fig. 1. This odd fact is due to the sensitivity of the Voronoi diagram and medial axis structure to the order of continuity of the boundary curve [12]. In particular,

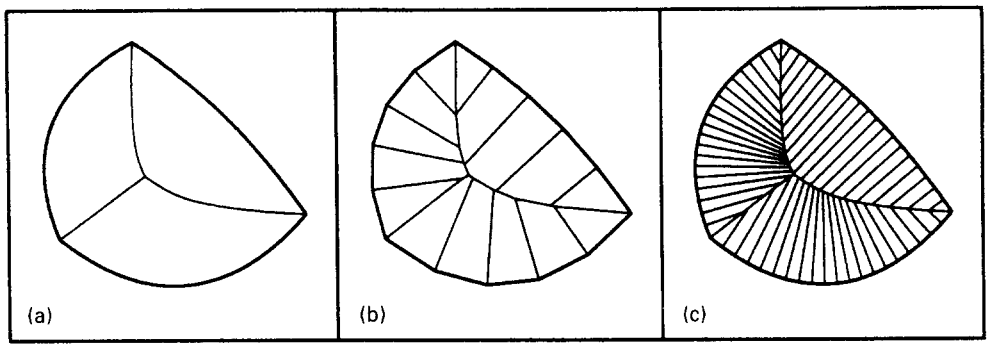

Fig. 1. Difference between (a) the true Voronoi diagram of a planar domain bounded by free-form curve segments, and that computed from piecewise-linear boundary approximations with (b) 15 segments and (c) 60 segments.

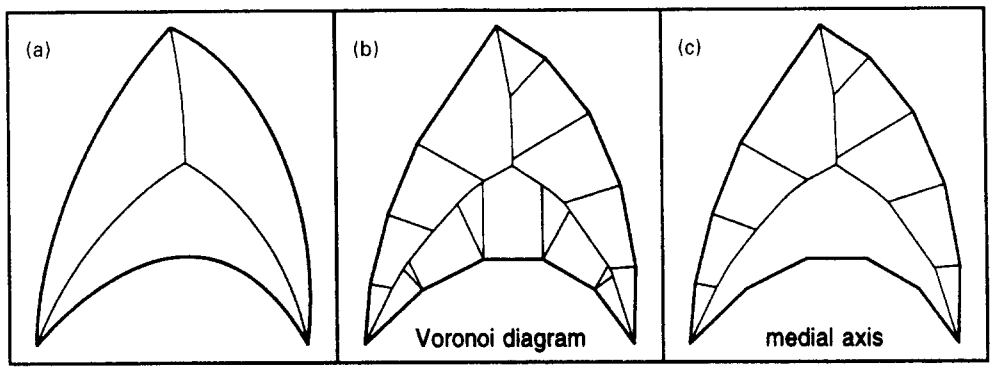

Fig. 2. A curved shape, for which the Voronoi diagram and medial axis are identical (a), but differ in (b) and (c) for a polygonal approximation thereof.

the presence of G^0 junctures between approximating elements to a smooth boundary segment incurs edges in the Voronoi diagram/medial axis that are absent from the exact structure. Note also that the Voronoi diagram and medial axis may be identical for the exact boundary, but different for the approximate boundary (see Fig. 2).

Thus, in computing the Voronoi diagram or medial axis for domains with free-form boundary curves, the computation *must* employ the exact analytic curve descriptions in order to ensure topologically correct results.

2.3. Distance functions and bisectors

In order to give a reasonably self-contained presentation, we begin by briefly reviewing some basic facts concerning distance functions and bisectors (the reader may consult [16, 18] for complete details).

1. The distance of a point $\boldsymbol{q}$ from a regular curve $\boldsymbol{r}(u) = (X(u), Y(u))$ for $u \in [0,1]$ is defined by

$$\operatorname{dist}(\boldsymbol{q}, \boldsymbol{r}(u)) = \min_{u \in [0,1]} |\boldsymbol{q} - \boldsymbol{r}(u)|. \tag{1}$$

2. Given the point $\boldsymbol{q} = (a, b)$ and the degree-n polynomial curve $\boldsymbol{r}(u) = (X(u), Y(u))$ for $u \in [0, 1]$, let $u_1, \ldots, u_N$ be the odd-multiplicity roots on $(0, 1)$ of the polynomial

$$P_\perp(u) = [a - X(u)]X'(u) + [b - Y(u)]Y'(u) \tag{2}$$

of degree $2n - 1$, and let $u_0 = 0$ and $u_{N+1} = 1$. The distance function (1) may then be expressed as

$$\operatorname{dist}(\boldsymbol{q}, \boldsymbol{r}(u)) = \min_{0 \leqslant k \leqslant N+1} |\boldsymbol{q} - \boldsymbol{r}(u_k)| . \tag{3}$$

An analogous formulation holds [16] for a rational curve $\boldsymbol{r}(u)$.

3. If the minimum value in (3) occurs for $k = m$, we call $\boldsymbol{r}(u_m)$ a *footpoint* of $\boldsymbol{q}$ on the curve $\boldsymbol{r}(u)$ – it is an *interior* footpoint if $1 \leqslant m \leqslant N$, and a *terminal* footpoint if $m = 0$ or $N + 1$.
4. The bisector of two curves, $\boldsymbol{r}(u)$ for $u \in [0, 1]$ and $\boldsymbol{s}(v)$ for $v \in [0, 1]$, is the set of points that are equidistant from those curves – i.e., it is the point set

$$\{\boldsymbol{q} \mid \operatorname{dist}(\boldsymbol{q}, \boldsymbol{r}(u)) = \operatorname{dist}(\boldsymbol{q}, \boldsymbol{s}(v))\} . \tag{4}$$

5. The *self-bisector* of a curve $\boldsymbol{r}(u)$ for $u \in [0, 1]$ is the closure of the set of points having (at least) two distinct footpoints on that curve – i.e., it is the closure of the point set

$$\{\boldsymbol{q} \mid \operatorname{dist}(\boldsymbol{q}, \boldsymbol{r}(u)) = |\boldsymbol{q} - \boldsymbol{r}(u_1)| = |\boldsymbol{q} - \boldsymbol{r}(u_2)| \text{ with } u_1 \neq u_2\} . \tag{5}$$

3. Voronoi diagrams

Our Voronoi diagram algorithm, to be outlined in Section 4 below, proceeds in an incremental manner by introducing one boundary segment at a time. This approach necessitates defining Voronoi diagrams not only for the boundaries of planar domains, but also for arbitrary sets of curve segments (which do not necessarily enclose a domain). The reasons for this will become apparent in Section 4. Clearly, the ability to define and compute Voronoi diagrams for arbitrary sets of curve segments subsumes the case of domain boundaries.

Definition 3.1. Let $\{s_1, \ldots, s_M\}$, with $M \geqslant 1$, be a subset of the N curve segments that comprise the boundary S of a planar domain D, and let $S_M = s_1 \cup \cdots \cup s_M \subseteq S$. Then:

(a) the *Voronoi region* $\mathrm{VR}(s_i)$ of boundary segment s_i, with respect to S_M, is the area defined by

$$\{\boldsymbol{q} \in \boldsymbol{R}^2 \mid \operatorname{dist}(\boldsymbol{q}, s_i) \leqslant \operatorname{dist}(\boldsymbol{q}, s_j) \quad \text{for } 1 \leqslant j \leqslant M,\ j \neq i\} ; \tag{6}$$

(b) the *Voronoi polygon*[3] $\mathrm{VP}(s_i)$ of segment s_i, with respect to S_M, is the boundary of $\mathrm{VR}(s_i)$;

(c) the *Voronoi diagram* $\mathrm{VD}(S_M)$ of the set of segments S_M is defined by

$$\mathrm{VD}(S_M) = \bigcup_{i=1}^{M} \mathrm{VP}(s_i) . \tag{7}$$

[3] It is customary to call $\mathrm{VP}(s_i)$ a 'polygon' although, in general, it has curved edges.

Remark 3.1. The Voronoi region $\mathrm{VR}(s_i)$ and polygon $\mathrm{VP}(s_i)$ are dependent on the segment set $S_M = s_1 \cup \cdots \cup s_M$ currently under consideration – they change, in general, upon introducing a new segment s_{M+1} and considering them with respect to $S_{M+1} = s_1 \cup \cdots \cup s_M \cup s_{M+1}$. When $M = 1$, the set S_1 consists of the single segment s_1, and we adopt the convention that $\mathrm{VR}(s_1)$ with respect to S_1 comprises the entire plane.

Remark 3.2. The Voronoi regions $\mathrm{VR}(s_i)$ and $\mathrm{VR}(s_j)$ of distinct segments, $i \neq j$, need not be disjoint. The 'overlap region' $\mathrm{VR}(s_i) \cap \mathrm{VR}(s_j)$ is just the set of points (if any) that are *equidistant* from segments s_i and s_j. In fact, the Voronoi region of s_i may overlap the Voronoi regions of several distinct segments in S_M. (By considering reflex[4] vertices as 'boundary elements' in their own right, Lee [29] avoids this overlap in the case of polygonal domains – we shall not accord special treatment to such boundary vertices, however.)

Remark 3.3. By Definition 3.1, for a domain with boundary S comprising N segments $s_1, \ldots, s_N$, the Voronoi regions of these segments partition the *entire* plane (not just the interior of S) into N regions. In other words, edges of the Voronoi polygons (and of the Voronoi diagram) that lie both *interior* and *exterior* to S are included in our definitions. If all the exterior edges are deleted, the 'interior' Voronoi diagram of S results – similarly, if all interior edges are deleted, the 'exterior' Voronoi diagram remains (other authors – e.g., Lee [29] – have employed the term 'Voronoi diagram' synonymously with the *interior* Voronoi diagram).

The boundaries of the Voronoi regions are evidently loci of points that are equidistant from two distinct segments, s_i and s_j say, of the boundary. Thus, the edges of the Voronoi polygons are portions of curve/curve bisectors (subsets of which may actually be point/curve bisectors) for distinct boundary segments. The construction of the Voronoi polygons therefore requires robust methods for curve/curve bisector computations. The algorithms developed in our earlier studies [16–19] satisfy this need.

4. Voronoi diagram algorithm

We now establish set-theory foundations for our Voronoi diagram algorithm. A high-level description of this algorithm is given in Section 4.1, while Sections 4.2–4.4 address key theoretical issues that arise in its formulation. We defer detailed treatment of the computational issues to a companion paper [37].

The procedure commences with a boundary segment set containing just a single segment. Recall (Remark 3.1) that the Voronoi region of this segment with respect to itself is the entire plane. We then incrementally augment the boundary segment set, by introducing one additional boundary segment at a time, and we re-construct the Voronoi regions of each segment with respect to the augmented set. Note that introducing a single segment may alter any or all of the current Voronoi regions (with respect to the augmented set). When all the boundary segments have been incorporated

[4] Where the interior angle included by adjacent line segments is greater than π.

in this manner, with their Voronoi regions/polygons updated at each step, the Voronoi diagram of the entire boundary is simply the union of the final Voronoi polygons.

Let D be a planar domain with boundary S comprising N curve segments $s_1,\ldots,s_N$. Consider a subset $S_M = s_1 \cup \cdots \cup s_M$ of S, and let $\mathrm{VR}(s_1),\ldots,\mathrm{VR}(s_M)$ be the Voronoi regions of these M segments with respect to S_M. If a new segment s_{M+1} is introduced, these regions are no longer the Voronoi regions of the M segments with respect to $S_{M+1} = s_1 \cup \cdots \cup s_{M+1}$. This is because each point in some (possibly null) subset of the Voronoi region $\mathrm{VR}(s_i)$ with respect to S_M is closer to s_{M+1} than to s_i, for $i = 1,\ldots,M$. Deleting these subsets from the 'old' Voronoi regions, $\mathrm{VR}(s_i)$ with respect to S_M, yields the 'new' Voronoi regions, $\mathrm{VR}(s_i)$ with respect to S_{M+1}.

The following proposition indicates how the current Voronoi regions are updated upon introducing a new boundary segment s_{M+1}, and also how the Voronoi region of the new segment (with respect to S_{M+1}) is determined:

Proposition 4.1. Let $S_M = s_1 \cup \cdots \cup s_M$ be a subset of the curve segments comprising the boundary S of a planar domain D, and let $\mathrm{VR}(s_i)$ denote the Voronoi region of segment s_i with respect to S_M, for $1 \leqslant i \leqslant M$. Introducing an additional segment s_{M+1}, and setting $S_{M+1} = s_1 \cup \cdots \cup s_{M+1}$, the bisector of s_i and s_{M+1} partitions $\mathrm{VR}(s_i)$ into three disjoint subsets such that:

1. $\mathrm{V}_<(s_i)$ is the subset of points in $\mathrm{VR}(s_i)$ closer to s_i than to s_{M+1};
2. $\mathrm{V}_=(s_i)$ is the subset of points in $\mathrm{VR}(s_i)$ equidistant from s_i and s_{M+1};
3. $\mathrm{V}_>(s_i)$ is the subset of points in $\mathrm{VR}(s_i)$ closer to s_{M+1} than to s_i.

Then, for $1 \leqslant i \leqslant M$, we have

$$\mathrm{VR}(s_i) \text{ w.r.t. } S_{M+1} = \mathrm{VR}(s_i) \text{ w.r.t. } S_M \; - \; V_>(s_i), \tag{8}$$

while the Voronoi region of the newly-introduced segment is given by

$$\mathrm{VR}(s_{M+1}) \text{ w.r.t. } S_{M+1} = \bigcup_{i=1}^{M} \mathrm{VR}(s_i) \text{ w.r.t. } S_M \; - \; V_<(s_i). \tag{9}$$

Proof. Let $\boldsymbol{q} \in \mathrm{VR}(s_i)$ w.r.t. $S_M - V_>(s_i)$. Then $\mathrm{dist}(\boldsymbol{q},s_i) \leqslant \mathrm{dist}(\boldsymbol{q},s_j)$ for $1 \leqslant j \neq i \leqslant M$ by the definition of $\mathrm{VR}(s_i)$ w.r.t. S_M. Moreover, $\mathrm{dist}(\boldsymbol{q},s_i) \leqslant \mathrm{dist}(\boldsymbol{q},s_{M+1})$ by the definition of $V_>(s_i)$. Thus $\boldsymbol{q} \in \mathrm{VR}(s_i)$ w.r.t. S_{M+1}, and we infer that $\mathrm{VR}(s_i)$ w.r.t. $S_M - V_>(s_i) \subseteq \mathrm{VR}(s_i)$ w.r.t. S_{M+1}. Conversely, let $\boldsymbol{q} \in \mathrm{VR}(s_i)$ w.r.t. S_{M+1}. Then $\mathrm{dist}(\boldsymbol{q},s_i) \leqslant \mathrm{dist}(\boldsymbol{q},s_j)$ for $1 \leqslant j \neq i \leqslant M$, and hence $\boldsymbol{q} \in \mathrm{VR}(s_i)$ w.r.t. S_M. Moreover, $\mathrm{dist}(\boldsymbol{q},s_i) \leqslant \mathrm{dist}(\boldsymbol{q},s_{M+1})$, so that $\boldsymbol{q} \notin V_>(s_i)$. Hence $\boldsymbol{q} \in \mathrm{VR}(s_i)$ w.r.t. $S_M - V_>(s_i)$, and we infer that $\mathrm{VR}(s_i)$ w.r.t. $S_{M+1} \subseteq \mathrm{VR}(s_i)$ w.r.t $S_M - V_>(s_i)$. This completes the proof of expression (8) in the proposition.

Suppose that $\boldsymbol{q} \in \mathrm{VR}(s_{M+1})$ w.r.t. S_{M+1}. Then $\mathrm{dist}(\boldsymbol{q},s_{M+1}) \leqslant \mathrm{dist}(\boldsymbol{q},s_i)$ for $1 \leqslant i \leqslant M$, by the definition of $\mathrm{VR}(s_{M+1})$ w.r.t. S_{M+1}. We now assume that $\boldsymbol{q} \notin V_=(s_i) \cup V_>(s_i)$ for $1 \leqslant i \leqslant M$. Then $\mathrm{dist}(\boldsymbol{q},s_{M+1}) \neq \mathrm{dist}(\boldsymbol{q},s_i)$ and $\mathrm{dist}(\boldsymbol{q},s_{M+1}) \not< \mathrm{dist}(\boldsymbol{q},s_i)$, and therefore $\mathrm{dist}(\boldsymbol{q},s_{M+1}) > \mathrm{dist}(\boldsymbol{q},s_i)$, for $1 \leqslant i \leqslant M$. Since we have arrived at a contradiction, the assumption must be false. Hence, there is an i such that $\boldsymbol{q} \in V_=(s_i) \cup V_>(s_i)$, and we have

$$\mathrm{VR}(s_{M+1}) \text{ w.r.t. } S_{M+1} \subseteq \bigcup_{i=1}^{M} V_=(s_i) \cup V_>(s_i). \tag{10}$$

Now, suppose that $\boldsymbol{q} \in \bigcup_{i=1}^{M} V_{=}(s_i) \cup V_{>}(s_i)$, so $\boldsymbol{q} \in V_{=}(s_i) \cup V_{>}(s_i)$ for some i. Then $\text{dist}(\boldsymbol{q}, s_i) \leqslant \text{dist}(\boldsymbol{q}, s_j)$ for $1 \leqslant j \neq i \leqslant M$, since $\boldsymbol{q}$ lies in $\text{VR}(s_i)$ w.r.t. S_M. Furthermore, $\text{dist}(\boldsymbol{q}, s_{M+1}) \leqslant \text{dist}(\boldsymbol{q}, s_i)$ by the definition of $V_{>}(s_i)$ and $V_{=}(s_i)$. Hence $\text{dist}(\boldsymbol{q}, s_{M+1}) \leqslant \text{dist}(\boldsymbol{q}, s_j)$ for $1 \leqslant j \leqslant M$, i.e., $\boldsymbol{q} \in \text{VR}(s_{M+1})$ w.r.t. S_{M+1}, and we infer that

$$\bigcup_{i=1}^{M} V_{=}(s_i) \cup V_{>}(s_i) \subseteq \text{VR}(s_{M+1}) \text{ w.r.t. } S_{M+1}. \tag{11}$$

But since $V_{<}(s_i)$, $V_{=}(s_i)$, and $V_{>}(s_i)$ are disjoint subsets partitioning $\text{VR}(s_i)$ w.r.t. S_M, for $1 \leqslant i \leqslant M$ we have

$$V_{=}(s_i) \cup V_{>}(s_i) = \text{VR}(s_i) \text{ w.r.t. } S_M - V_{<}(s_i) \tag{12}$$

Expression (9) can be directly inferred from (10)–(12), and hence the proof of the proposition is complete. □

4.1. Outline of algorithm

We now outline our Voronoi diagram algorithm, based on Proposition 4.1:

input: boundary $S = s_1 \cup \cdots \cup s_N$ of domain D.
1. set $S_1 = s_1$ and $\text{VR}(s_1)$ w.r.t. $S_1 = \mathbb{R}^2$;
2. for $M = 1, \ldots, N-1$ do
   a. introduce s_{M+1}, set $S_{M+1} = S_M \cup s_{M+1}$, and update Voronoi regions of $s_1, \ldots, s_M$ as follows:
   b. for $i = 1, \ldots, M$ do
      i. construct the bisector of s_{M+1} with s_i;
      ii. construct the subsets $V_{<}(s_i)$ and $V_{>}(s_i)$ of $\text{VR}(s_i)$ w.r.t. S_M defined in Proposition 4.1;
      iii. construct $\text{VR}(s_i)$ w.r.t. S_{M+1} using (8);
      end do
   c. construct $\text{VR}(s_{M+1})$ w.r.t. S_{M+1} using (9);
   end do
3. define $\text{VD}(S) = \cup_{i=1}^{N} \text{VP}(s_i)$ w.r.t. S_N;

output : Voronoi diagram $\text{VD}(S)$ of boundary.

The key steps in the implementation of this algorithm are evidently (i) the construction of the curve/curve bisectors; and (ii) the partitioning of Voronoi regions, by these bisectors, into the subsets defined in Proposition 4.1. The curve/curve bisector construction has been dealt with in detail elsewhere [18, 19]. We now turn our attention to the Voronoi region paritioning problem.

4.2. Partitioning of Voronoi regions

To perform the Boolean operations in (8) and (9), a complete description of the *oriented* boundaries[5] of $\text{VR}(s_i)$ w.r.t. S_M, and of $V_{>}(s_i)$ and $V_{<}(s_i)$, for $1 \leqslant i \leqslant M$ is necessary and sufficient. Now

[5] If the boundary of a regular plane set is oriented in a consistent manner, its interior lies on the 'same side' (left/right) as the boundary is traversed in the sense of its orientation.

the oriented boundary of $\mathrm{VR}(s_i)$ w.r.t. S_M is already known from prior computations. Consequently, it suffices to construct the oriented boundaries of $V_>(s_i)$ and $V_<(s_i)$ to allow for the evaluation of expressions (8) and (9).

Toward this end, we define $\overline{V}_<(s_i, s_{M+1})$ and $\overline{V}_>(s_i, s_{M+1})$ by

$$\begin{aligned}\overline{V}_<(s_i, s_{M+1}) &= \{\, \boldsymbol{q} \in \mathbb{R}^2 \mid \mathrm{dist}(\boldsymbol{q}, s_i) < \mathrm{dist}(\boldsymbol{q}, s_{M+1}) \,\},\\ \overline{V}_>(s_i, s_{M+1}) &= \{\, \boldsymbol{q} \in \mathbb{R}^2 \mid \mathrm{dist}(\boldsymbol{q}, s_i) > \mathrm{dist}(\boldsymbol{q}, s_{M+1}) \,\},\end{aligned} \tag{13}$$

and we then have

$$\begin{aligned}V_<(s_i) &= \mathrm{VR}(s_i) \text{ w.r.t. } S_M \cap \overline{V}_<(s_i, s_{M+1}),\\ V_>(s_i) &= \mathrm{VR}(s_i) \text{ w.r.t. } S_M \cap \overline{V}_>(s_i, s_{M+1}).\end{aligned} \tag{14}$$

To evaluate expressions (14) we shall need to: (i) construct the boundaries of the sets $\overline{V}_<(s_i, s_{M+1})$ and $\overline{V}_>(s_i, s_{M+1})$, and (ii) compute all the points of intersection of the boundaries of $\overline{V}_<(s_i, s_{M+1})$ and $\overline{V}_>(s_i, s_{M+1})$ with the boundary of $\mathrm{VR}(s_i)$ w.r.t. S_M. We address the former issue here, and defer discussion of the latter problem to the following section.

By definition, each point $\boldsymbol{q}$ on the boundary of either $\overline{V}_<(s_i, s_{M+1})$ or $\overline{V}_>(s_i, s_{M+1})$ is equidistant from both s_i and s_{M+1}, i.e., we have $\mathrm{dist}(\boldsymbol{q}, s_i) = \mathrm{dist}(\boldsymbol{q}, s_{M+1})$. Hence, the boundary segments of these sets must be portions of the bisector of s_i and s_{M+1}. When s_i and s_{M+1} have no common points, the *entire* bisector of s_i and s_{M+1}, which is a continuous locus [18], bounds *both* $\overline{V}_<(s_i, s_{M+1})$ *and* $\overline{V}_>(s_i, s_{M+1})$. This is because, in a neighborhood of each bisector point, all points that lie locally on one side[6] of the bisector are closer to s_i than s_{M+1}, while those that lie locally on the other side are closer to s_{M+1} than to s_i, in this instance. Hence, constructing the boundaries of $\overline{V}_<(s_i, s_{M+1})$ and $\overline{V}_>(s_i, s_{M+1})$ reduces to simply computing the bisector of s_i and s_{M+1}, and the algorithm in [18] can be used to accomplish this.

When the segments s_i and s_{M+1} share a common endpoint, however, their bisector is no longer simply a one-dimensional locus – it is of mixed dimension, i.e., it comprises a one-dimensional locus and a convex two-dimensional region [19]. In this case, the boundaries of $\overline{V}_<(s_i, s_{M+1})$ and of $\overline{V}_>(s_i, s_{M+1})$ are *subsets* of the boundary[7] of the bisector of s_i and s_{M+1}. To identify these subsets, we must briefly review the nature of the bisector of curves that share a common endpoint (further details may be found in [19]).

4.3. *Bisector of curves with a common endpoint*

Let $\boldsymbol{p}$ be the common endpoint of the boundary segments s_i and s_{M+1}. For the purposes of the ensuing discussion, we shall represent these segments by the parametric curves $\boldsymbol{r}(u)$ for $u \in [0, 1]$ and

[6] Points in a neighborhood of a tangent-continuous bisector point $\boldsymbol{q}$ are separated into left and right 'sides' by the tangent at $\boldsymbol{q}$. If $\boldsymbol{q}$ is an exceptional point, the limiting tangents before and after $\boldsymbol{q}$ are considered to divide its neighborhood into two (wedge-shaped) sides.

[7] The boundary of the bisector of s_i and s_{M+1} is the union of the one-dimensional locus and the boundary of the two-dimensional region. Further, the boundaries of $\overline{V}_<(s_i, s_{M+1})$ and $\overline{V}_>(s_i, s_{M+1})$ together form the boundary of the bisector of s_i and s_{M+1}.

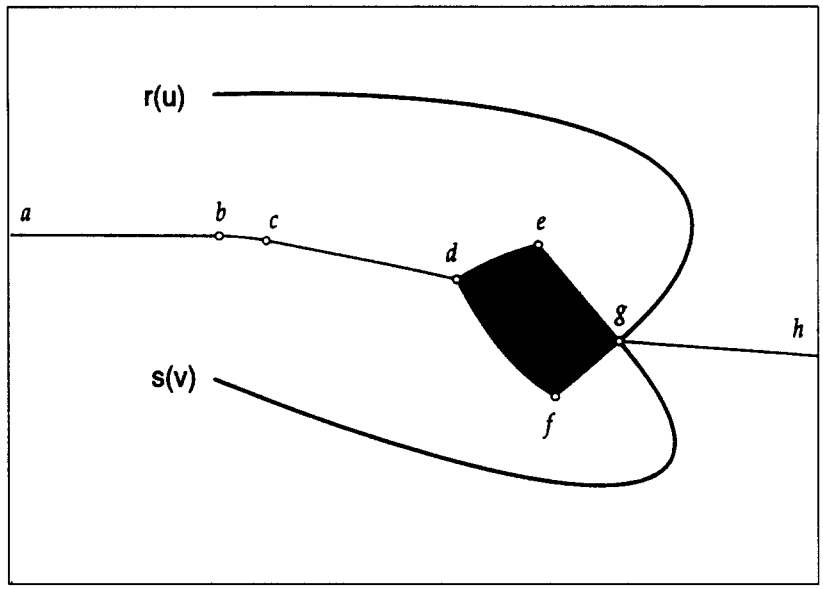

Fig. 3. The bisector of curves $r(u)$ and $s(v)$ that meet with C^0 continuity, comprising the shaded region $B_1 \cup B_2 \cup B_3$ and the locus B_0 consisting of *abcd* and *gh*. Here, *deg* is the subset a_r of the boundary of A_r that belongs to the boundary of $A_r \cap A_s$, while *dfg* is the subset a_s of the boundary of A_s which forms the remainder of the boundary of $A_r \cap A_s$.

$s(v)$ for $v \in [0,1]$, respectively. Let B be the set of bisector points satisfying (4), and suppose $\boldsymbol{q}$ is a point of B with footpoint parameter values u_m and v_m on $\boldsymbol{r}(u)$ and $\boldsymbol{s}(v)$, respectively. Then, according to the nature of these footpoints, we may decompose B into the following four components:

0. the set B_0 of points $\boldsymbol{q}$ that have footpoints $\boldsymbol{r}(u_m) \neq \boldsymbol{p}$ on $\boldsymbol{r}(u)$ and $\boldsymbol{s}(v_m) \neq \boldsymbol{p}$ on $\boldsymbol{s}(v)$;
1. the set B_1 of points $\boldsymbol{q}$ that have footpoints $\boldsymbol{r}(u_m) = \boldsymbol{p}$ on $\boldsymbol{r}(u)$ *and* $\boldsymbol{s}(v_m) \neq \boldsymbol{p}$ on$\boldsymbol{s}(v)$;
2. the set B_2 of points $\boldsymbol{q}$ that have footpoints $\boldsymbol{r}(u_m) \neq \boldsymbol{p}$ on $\boldsymbol{r}(u)$ and $\boldsymbol{s}(v_m) = \boldsymbol{p}$ *on* $\boldsymbol{s}(v)$;
3. the set B_3 of points $\boldsymbol{q}$ that have footpoints $\boldsymbol{r}(u_m) = \boldsymbol{p}$ on $\boldsymbol{r}(u)$ and $\boldsymbol{s}(v_m) = \boldsymbol{p}$ on $\boldsymbol{s}(v)$.

The boundary of B may be obtained as the boundary of $B_0 \cup B_1 \cup B_2 \cup B_3$. The set B_0 is the one-dimensional component of B [19] – the neighborhood of any point $\boldsymbol{q} \in B_0$ contains points that are closer to s_i than to s_{M+1} *and* points that are closer to s_{M+1} than to s_i, lying on opposite sides (locally) of B_0. Consequently, B_0 bounds both $\overline{V}_<(s_i, s_{M+1})$ and $\overline{V}_>(s_i, s_{M+1})$. The curve/curve bisector algorithm described in [18] can be used to compute B_0. However, since this algorithm implicitly assumes that $\boldsymbol{r}(u)$ and $\boldsymbol{s}(v)$ have distinct endpoints, it will fail to yield the sets B_1, B_2, B_3.

A separate procedure is therefore needed to construct these sets or, more specifically, $B_1 \cup B_2 \cup B_3$. Toward this end, define A_r to be the point/curve bisector of $\boldsymbol{p}$ and $\boldsymbol{r}(u)$ for $u \in [0,1]$ and A_s to be that of $\boldsymbol{p}$ and $\boldsymbol{s}(v)$ for $v \in [0,1]$. It was shown in Proposition 5.1 of [19] that $A_r \cap A_s = B_1 \cup B_2 \cup B_3$, and the boundary of $A_r \cap A_s$ is thus identical to that of $B_1 \cup B_2 \cup B_3$. Note that the point/curve bisectors A_r and A_s are not one-dimensional loci, but rather convex *two-dimensional* subsets of the

plane [19]; these sets are specified by their oriented boundaries. Consequently, the bisector of two curves having a common endpoint is of mixed dimension – as illustrated in Fig. 3.

In the following discussion, let a_r and a_s denote the set of all segments contained in A_r and A_s, respectively, that bound $A_r \cap A_s$ (see Fig. 3). Note that (i) points lying exterior to the boundary of A_r are closer to $\boldsymbol{r}(u)$ than to $\boldsymbol{p}$; and (ii) those lying on the boundary and in the interior of A_r are equidistant from $\boldsymbol{r}(u)$ and $\boldsymbol{p}$. Thus, segments in a_r that contribute to the boundary of $A_r \cap A_s = B_1 \cup B_2 \cup B_3$ are also boundary segments of $\overline{V}_<(s_i, s_{M+1})$. Moreover, these segments are *not* part of the boundary of $\overline{V}_>(s_i, s_{M+1})$. Similarly, segments in a_s contributing to the remainder of the boundary of $A_r \cap A_s$ are part of the boundary of $\overline{V}_>(s_i, s_{M+1})$, exclusively.

In this manner, every segment of the boundary of the bisector B of s_i and s_{M+1} is associated with the boundary of either $\overline{V}_<(s_i, s_{M+1})$ or $\overline{V}_>(s_i, s_{M+1})$, and we may conclude that, when s_i and s_{M+1} share a common endpoint,

$$\begin{aligned} &\text{boundary of } \overline{V}_<(s_i, s_{M+1}) = B_0 \cup a_r\,, \\ &\text{boundary of } \overline{V}_>(s_i, s_{M+1}) = B_0 \cup a_s\,. \end{aligned} \tag{15}$$

Finally, in addition to identifying the boundary segments of $\overline{V}_<(s_i, s_{M+1})$ and $\overline{V}_>(s_i, s_{M+1})$, we also need to orient them properly. This requires two additional steps. First, in order to ensure that the boundaries of $\overline{V}_<(s_i, s_{M+1})$ and $\overline{V}_>(s_i, s_{M+1})$ can be traversed continuously in a consistent sense, their segments must be arranged in sequence, such that the start point of each boundary segment coincides with the end point of its predecessor, and the end point coincides with the start point of its successor. Second, we must ensure that the 'interiors' of $\overline{V}_<(s_i, s_{M+1})$ and $\overline{V}_>(s_i, s_{M+1})$ consistently lie (locally) to the left as their boundaries are traversed.

4.4. Nature of bifurcation points

To determine the sets (14), we must evaluate the boundaries of $\overline{V}_<(s_i, s_{M+1})$ and $\overline{V}_>(s_i, s_{M+1})$, and compute all intersection points of these boundaries with the Voronoi polygon of s_i w.r.t. S_M. These intersection points are called bifurcation points or three-prong points [12], or simply bifurcations, of the Voronoi diagram – they correspond to points with *three*[8] footpoints on the boundary. Since (parts of) the boundaries of $\overline{V}_<(s_i, s_{M+1})$, $\overline{V}_>(s_i, s_{M+1})$, and $\mathrm{VR}(s_i)$ w.r.t. S_M must be approximated, the bifurcation-point coordinates determined by standard curve intersection algorithms [39] may likewise be approximate. We now classify the bifurcations, and identify those that need 'refinement' so as to have essentially *exact* coordinates.

According to the nature of their three footpoints on the boundary, we can classify bifurcation points into the following three categories:

(1) those that have three footpoints on a single boundary segment s_i;
(2) those that have two footpoints points on a single boundary segment s_i, and the third footpoint on a different segment s_j;

[8] Points with four or more footpoints arise only under exceptional circumstances – for brevity, we shall not address them here.

(3) those that have each of their three footpoints on three distinct boundary segments s_i, s_j, s_k.

Bifurcations of type (1) must have (at least) one terminal[9] footpoint on s_i. Now suppose s_i is represented by the parametric curve $\boldsymbol{r}(u)$ for $u \in [0,1]$. Then, depending on whether the bifurcation point has a terminal footpoint at either $\boldsymbol{r}(0)$ or at $\boldsymbol{r}(1)$, it is a self-intersection [16] point of the untrimmed point/curve bisector of either $\boldsymbol{r}(0)$ and s_i or $\boldsymbol{r}(1)$ and s_i, respectively. Since the point/curve bisector of $\boldsymbol{r}(0)$ and s_i is constructed at the time the bisector of s_{i-1} and s_i is computed,[10] all bifurcation points of type (1) lying on this point/curve bisector are found at that time. Similarly, all bifurcation points of type (1) lying on the bisector of $\boldsymbol{r}(1)$ and s_i are found while constructing the bisector of s_i and s_{i+1}. In this manner all type (1) bifurcations will be precisely located, and no refinement of their coordinates is necessary.

Bifurcations of type (2) are the 'exceptional' (i.e., *critical* or *transition*) points [18] on the curve/curve bisector of segments s_i and s_j. Such points are explicitly located while computing this curve/curve bisector [18], and thus do not require further consideration. Bifurcations of type (3), however, must be located during construction of the Voronoi diagram. Based on the nature of their footpoints on s_i, s_j, s_k we can further differentiate among type (3) bifurcation points as follows:

(3a) those with *terminal* footpoints on all three of the segments s_i, s_j, s_k;

(3b) those with *terminal* footpoints on two of the segments s_i, s_j, s_k and an *interior* footpoint on the third;

(3c) those with *interior* footpoints on two of the segments s_i, s_j, s_k and a *terminal* footpoint on the third;

(3d) those with *interior* footpoints on all three of the segments s_i, s_j, s_k.

Bifurcations of type (3a) are points of concurrency of three linear segments in the Voronoi diagram, while those of type (3b) correspond to the common intersection of a linear segment and two rational point/curve bisectors. The locations of such bifurcation points computed by standard curve-intersection algorithms are essentially exact, and require no further refinement.

Bifurcations of type (3c) in the Voronoi diagram arise where two rational (point/curve) and one non-rational (curve/curve) bisector segments meet, while those of type (3d) are the intersections of three non-rational segments. Since the non-rational bisector segments must be approximated by Hermite interpolants to discrete data, the bifurcation-point coordinates computed as their intersections are inherently approximate. A means of refining these bifurcation points so as to obtain essentially exact coordinates is required. A Newton–Raphson scheme which receives the approximate coordinates of type (3c) and (3d) bifurcation points as input, and returns the true bifurcation-point coordinates is described in the companion paper [37].

5. Illustrative example

We illustrate the working of our algorithm by a step-by-step Voronoi diagram construction for the simple three-segment boundary shown in Fig. 7 below. The boundary segments are polynomial or rational curves $\boldsymbol{r}_1(u)$, $\boldsymbol{r}_2(u)$, $\boldsymbol{r}_3(u)$ defined on $u \in [0,1]$. For brevity, we refer to them as s_1, s_2, s_3.

[9] We assume the boundary is composed of 'simple' segments (see Definition 4.2 in [19]) and hence no point may have three 'interior' footpoints on a *single* segment.

[10] We suppose that $\boldsymbol{r}(0)$ is the common endpoint of s_{i-1} and s_i, while $\boldsymbol{r}(1)$ is the common endpoint of s_i and s_{i+1}.

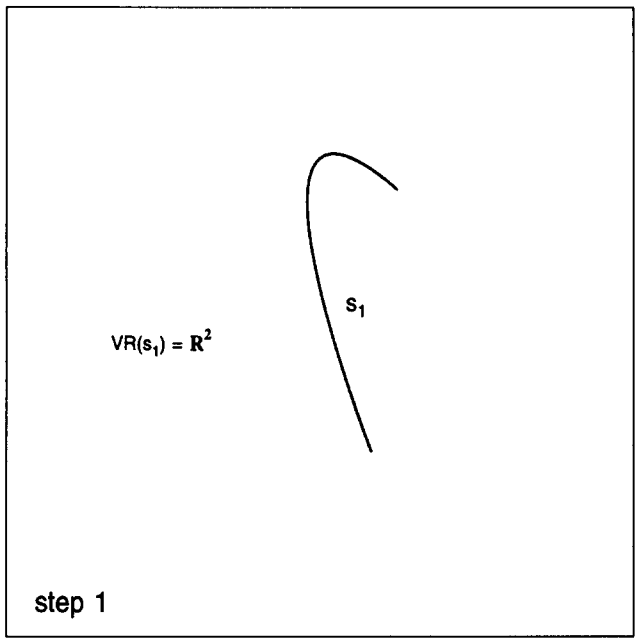

Fig. 4. The algorithm commences in step 1 with a single boundary segment s_1 comprising the set S_1, and by convention we have VR(s_1) w.r.t. $S_1 = \mathbb{R}^2$.

In the ensuing description we adopt the following convention. If $x, y, \ldots, z$ is a sequence of discrete points, joined by unique bisector segments, we denote the *open* region that lies to the left of the oriented locus $xy \ldots z$ by $\boldsymbol{R}(xy \ldots z)$. This encompasses all points up to, though not including, the bounding locus $xy \ldots z$. The *closed* region that lies to the left of $xy \ldots z$, which incorporates this bounding locus, is denoted by $\overline{\boldsymbol{R}}(xy \ldots z)$.

1. We initialize the boundary segment set by setting $S_1 = s_1$. The Voronoi region VR(s_1) w.r.t. S_1 is the entire plane (see Fig. 4).
2. A new segment s_2 is introduced, and we set $S_2 = s_1 \cup s_2$. The Voronoi region of s_1 w.r.t. S_2 is not the same as its Voronoi region w.r.t. S_1 (namely, $\mathbb{R}^2$). To construct the Voronoi region of s_1 w.r.t. S_2, and that of the new segment s_2, we do the following (see Fig. 5):
   (a) compute the bisector of the new segment s_2 and s_1;
   (b) partition VR(s_1) w.r.t. S_1 ($= \mathbb{R}^2$) into subsets $V_<(s_1)$ and $V_>(s_1)$ of points closer to s_1 than s_2, and closer to s_2 than s_1, respectively;
   (c) finally, construct VR(s_1) and VR(s_2) w.r.t. S_2 using (8) and (9).
   Thus, in Fig. 5, we have VR(s_1) w.r.t. $S_2 = \overline{\boldsymbol{R}}(hgfedba)$, while VR($s_2$) w.r.t. $S_2 = \overline{\boldsymbol{R}}(abcefgh)$. Note also that these two Voronoi regions are not disjoint – their 'overlap region,' bounded by *bcedb*, is the convex two-dimensional subset of the bisector of s_1 and s_2.
3. The final segment s_3 is introduced to give the complete boundary, $S_3 = s_1 \cup s_2 \cup s_3$. Again, the Voronoi regions of s_1 and s_2 w.r.t. S_2 must be updated to obtain their Voronoi regions w.r.t. S_3. We accomplish this by computing the bisector of the new segment s_3 with each of the existing segments s_1 and s_2, and then constructing the regions $V_<(s_j)$ and $V_>(s_j)$ for $j = 1, 2$, as discussed in step 2. Finally, using the Voronoi regions of s_1 and s_2 w.r.t. S_2 (from the preceding step), and

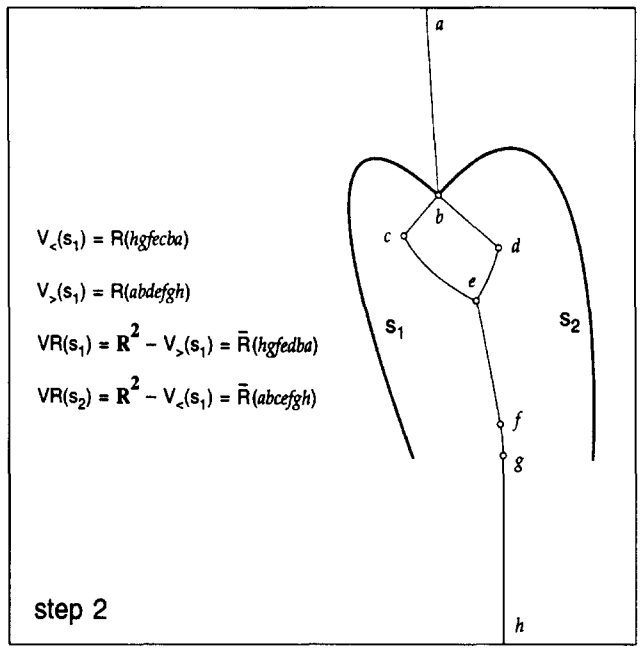

Fig. 5. In step 2, we partition VR(s_1) w.r.t. S_1 ($= \boldsymbol{R}^2$) into the subsets $V_<(s_1)$ and $V_>(s_1)$, whose points are closer to s_1 than s_2, and to s_2 than s_1, respectively. The Voronoi regions of s_1 and s_2 w.r.t. $S_2 = s_1 \cup s_2$ are also indicated in this figure. Here R($xy\ldots z$) and $\overline{\mathrm{R}}(xy\ldots z)$ denote, respectively, the *open* and *closed* regions lying to the left of the oriented curve $xy\ldots z$.

the $V_<(s_j)$, $V_>(s_j)$ computed in this step, we identify VR(s_1), VR(s_2), VR(s_3) w.r.t. S_3 through expressions (8) and (9). Thus, referring to Fig. 6, we have

VR(s_1) w.r.t. $S_3 = \overline{\boldsymbol{R}}(hnjiedba)$;
VR(s_2) w.r.t. $S_3 = \overline{\boldsymbol{R}}(abceiknh)$;
VR(s_3) w.r.t. $S_3 = \overline{\boldsymbol{R}}(mkijl)$.

Again, we note that VR(s_1), VR(s_2), VR(s_3) are mutually overlapping.

4. Finally, we may extract the *interior* Voronoi diagram by discarding all edges of the Voronoi diagram that lie outside the boundary curve (see Fig. 7). Alternately, we can extract the *exterior* Voronoi diagram by discarding all the Voronoi edges lying interior to the boundary.

6. Medial axis

We now focus our attention on the medial axis. In this and the following two sections, we give a formal definition of the medial axis, describe similarities and differences with the Voronoi diagram, and extend the algorithm of Section 4 to allow the medial axis to be constructed from the Voronoi diagram.

To define the medial axis, we introduce a slightly more general definition of the point/curve distance function (1) that encompasses composite curves:

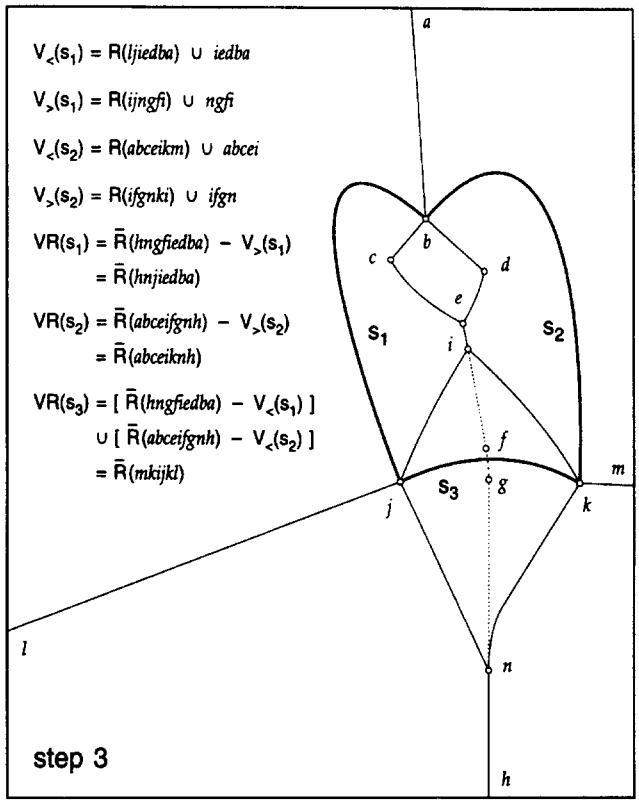

Fig. 6. In step 3, $V_<(s_1)$ and $V_>(s_1)$ are the subsets of VR(s_1) w.r.t. S_2 whose points are closer to s_1 than s_3, and to s_3 than s_1, respectively – similarly for the subsets $V_<(s_2)$ and $V_>(s_2)$ of VR(s_2) w.r.t. S_2. Note here that the dotted locus $ifgn$ is an edge of the Voronoi polygons of s_1 and s_2 w.r.t. S_2 (*not* w.r.t. S_3). The final Voronoi regions VR(s_1), VR(s_2), VR(s_3) w.r.t. S_3 are also indicated here.

Definition 6.1. Let $\boldsymbol{r}_1(u),\ldots,\boldsymbol{r}_N(u)$ for $u \in [0,1]$ be regular plane curves that comprise the boundary S of a planar domain D. Then the distance of a point $\boldsymbol{q} \in D$ from S is defined by

$$\operatorname{dist}(\boldsymbol{q},S) = \min_{1\leqslant i\leqslant N} \operatorname{dist}(\boldsymbol{q},\boldsymbol{r}_i(u)). \tag{16}$$

In terms of this distance function, we define the medial axis as follows:

Definition 6.2. The *medial axis* of the boundary S of a planar domain D is the closure of the set of points in D that have (at least) *two distinct footpoints* on S – i.e., it is the closure[11] of the point set

$$\{\boldsymbol{q} \in D \mid \exists \boldsymbol{p}_1,\boldsymbol{p}_2 \in S \text{ such that } \operatorname{dist}(\boldsymbol{q},S) = |\boldsymbol{q}-\boldsymbol{p}_1| = |\boldsymbol{q}-\boldsymbol{p}_2| \text{ with } \boldsymbol{p}_1 \neq \boldsymbol{p}_2\}. \tag{17}$$

We shall denote the medial axis of S by MA(S).

[11] By taking the *closure* of the set (17) we include its limit points, at which two formerly distinct footpoints on S coalesce into one. Such points correspond to centers of curvature for the vertices (i.e., points of extremum curvature) on S, and we consider them to have a footpoint of multiplicity 2 on S.

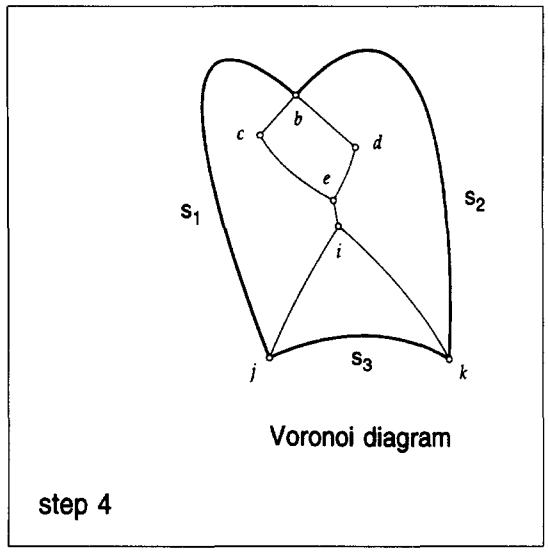

Fig. 7. In step 4 of the algorithm, the exterior Voronoi edges computed in step 3 are discarded to yield the *interior* Voronoi diagram. Note here that edges *bc* and *bd* are line segments; *ce* and *de* are *exact* rational point/curve bisector segments; and edges *ei*, *ij*, *ik* are Hermite approximants (satisfying a prescribed tolerance) to non-rational segments of curve/curve bisectors – namely, the bisectors of s_1 & s_2, of s_3 & s_1, and of s_2 & s_3, respectively.

Remark 6.1. A point $\boldsymbol{q}$ on the bisector of two boundary segments s_i and s_j has (at least) one footpoint on each of them. If these footpoints are distinct (namely, they are *not* a common endpoint of s_i and s_j), then $\boldsymbol{q}$ must belong to MA(S). But we know from Sections 3–5 that such points $\boldsymbol{q}$ also belong to VD(S). Hence, MA(S) and VD(S) possess many edges in common, and are intimately related. (Note, however, that unlike the Voronoi diagram, the medial axis is usually defined only in the *interior* of the domain D.)

By unambiguously characterizing the common edges of MA(S) and VD(S), we can partially construct one from the other. To complete the construction, we also need to give precise characterizations of the differences between the medial axis and Voronoi diagram. We address this in the following section.

7. Differences between VD and MA

Lee [29] has shown that the Voronoi diagram and medial axis of any convex polygon are identical, and that the medial axis of an arbitrary polygon is a *subset* of its Voronoi diagram. For reasons identical to those in the case of general polygons, the medial axes of piecewise-linear/circular boundaries are likewise subsets of their Voronoi diagrams. For domains bounded by free-form curve segments, however, neither the Voronoi diagram nor the medial axis of the boundary is, in general, a subset of the other. We now explore the reasons for this perhaps-unexpected result.

7.1. VD $\not\subseteq$ MA and MA $\not\subseteq$ VD

We first show that the Voronoi diagram is not a subset of the medial axis. In Section 4.3 we briefly reviewed the nature of the bisector of two curves that share a common endpoint. Now suppose B is a common edge of the Voronoi polygons of two boundary segments s_1 and s_2 that share an endpoint $\boldsymbol{p}$. Then B must be a subset of the bisector of s_1 and s_2. We decompose B into the subsets B_0, B_1, B_2, B_3 defined in Section 4.3. Points in B_3 have $\boldsymbol{p}$ as their only footpoint on each of s_1 and s_2. Thus, while such points belong to the Voronoi diagram, they cannot belong to the medial axis, since points on the latter must have (at least) two *distinct* footpoints on the boundary.[12] In fact, we may also argue that, excepting the points of B_3, all other points of B belong to the medial axis, since all points of B_0, B_1, B_2 satisfy the conditions in (17).

We thus conclude that, in general, the Voronoi diagram is *not* a subset of the medial axis. Specifically, edges of the Voronoi diagram whose constituent points have a unique footpoint on the boundary do not belong to the medial axis. Such edges are portions of the B_3 subsets of curve/curve bisectors for boundary segments that have a common endpoint.

Now consider an edge B of the medial axis (lying between bifurcations). Each interior point $\boldsymbol{q}$ of B has two footpoints, $\boldsymbol{p}_1$ and $\boldsymbol{p}_2$ say, on the domain boundary. Based on the nature of these footpoints, we can distinguish two types of medial axis edges (see Section 2.3):

(a) those for which $\boldsymbol{p}_1$ and $\boldsymbol{p}_2$ reside on *distinct* segments of the boundary – such edges are portions of *curve/curve bisectors*;
(b) those for which $\boldsymbol{p}_1$ and $\boldsymbol{p}_2$ reside on a *single* segment of the boundary – such edges are portions of *curve self-bisectors*.

Clearly, medial axis edges of type (b) cannot belong to the Voronoi diagram, since they are not equidistant from *distinct* boundary segments (see Section 3).

Hence we conclude that the medial axis of a domain is not, in general, contained within the Voronoi diagram of the domain boundary. Specifically, the medial axis generally contains edges corresponding to portions of the (interior) self-bisectors of individual boundary segments, which do not belong to the Voronoi diagram. A notable exception to this rule is the case of domains with piecewise-linear/circular boundaries: since linear and circular segments do not possess interior self-bisectors, the medial axis *is* a subset of the Voronoi diagram in this particular context.

7.2. Example

Fig. 8 illustrates these differences between the Voronoi diagram and medial axis (the derivation of the latter from the former is described in Section 8 below). Note the absence of Voronoi edges bc and bd from the medial axis, since points on these edges have b as their sole footpoint on the boundary. Conversely, the medial axis edges co and dp are absent from the Voronoi diagram, since both the footpoints of each point on these two edges lie on the interior of a single boundary segment – namely, s_1 and s_2, respectively.

7.3. Dependence of VD on boundary segmentation

In Section 1 we mentioned that the Voronoi diagram of a domain boundary depends on how the boundary is segmented, while the medial axis depends only on the *geometry* of the boundary. This

[12] Other than the limit points mentioned in the footnote to Definition 6.2.

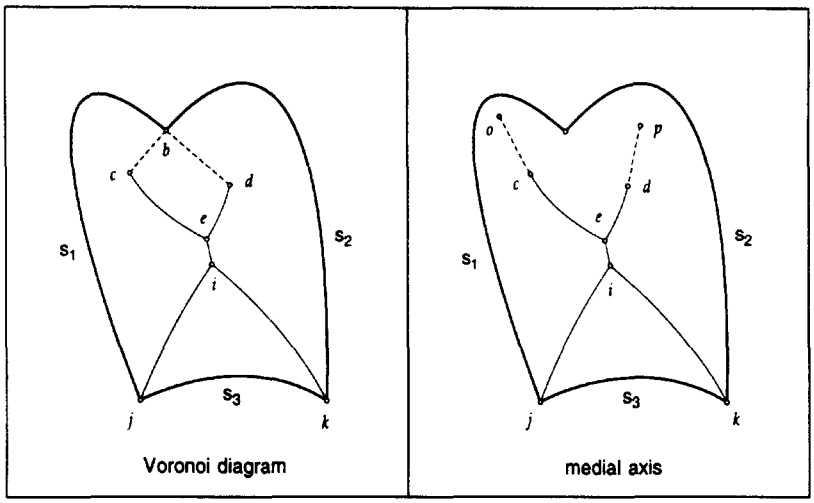

Fig. 8. Differences between (interior) Voronoi diagram and medial axis. The dotted Voronoi edges, on the left, have the common endpoint of segments s_1 and s_2 as their sole boundary footpoint, and hence do not belong to the medial axis. The dotted medial axes edges, on the right, are self-bisectors of boundary segments s_1 and s_2 – since each of their points have two footpoints on a single boundary segment, they do not belong to the Voronoi diagram.

phenomenon is illustrated in Fig. 9, where the boundary S of a planar domain is shown with two different segmentations, $S = r_1 \cup r_2 \cup r_3$ and $S = s_1 \cup s_2 \cup s_3$. Clearly, the Voronoi diagram of the former differs from that of the latter. The segments *eh* and *hg* in the Voronoi diagram of $r_1 \cup r_2 \cup r_3$ do not belong to the Voronoi diagram of $s_1 \cup s_2 \cup s_3$, since each interior point of these segments is closer to s_3 than to either s_1 or s_2. Similarly, each interior point of the segment *cd* in the Voronoi diagram of $s_1 \cup s_2 \cup s_3$ is closer to r_2 than to either r_1 or r_3, and consequently it does not belong to the Voronoi diagram of $S = r_1 \cup r_2 \cup r_3$.

Now segment *hg* does not belong to the medial axis of $S = r_1 \cup r_2 \cup r_3$, since points on *hg* have *g* as their only footpoint on S. Likewise, segment *cd* does not belong to the medial axis of S. To complete the medial axes, we need to combine the interior self-bisectors of the boundary segments with the results of the above removal operations. The boundary segments r_1, r_2 and s_1, s_2 do not have interior self-bisectors, while the interior self-bisectors of r_3 and s_3 are the loci *hf* and *ef*, respectively. Thus, the resulting medial axes of $S = r_1 \cup r_2 \cup r_3$ and $S = s_1 \cup s_2 \cup s_3$ are identical.

8. Medial axis algorithm

We construct the medial axis from the Voronoi diagram by (i) deleting edges of the latter that do not belong to the former, and (ii) adding medial axis edges that are absent from the Voronoi diagram, as discussed in Section 7. Trivially, no edge of the exterior Voronoi diagram can belong to the medial axis, and all such edges are therefore initially discarded.

In Section 7 we noted that those Voronoi edges whose points have a single distinct footpoint on the boundary (which are portions of bisectors of curve segments that have a common endpoint) are

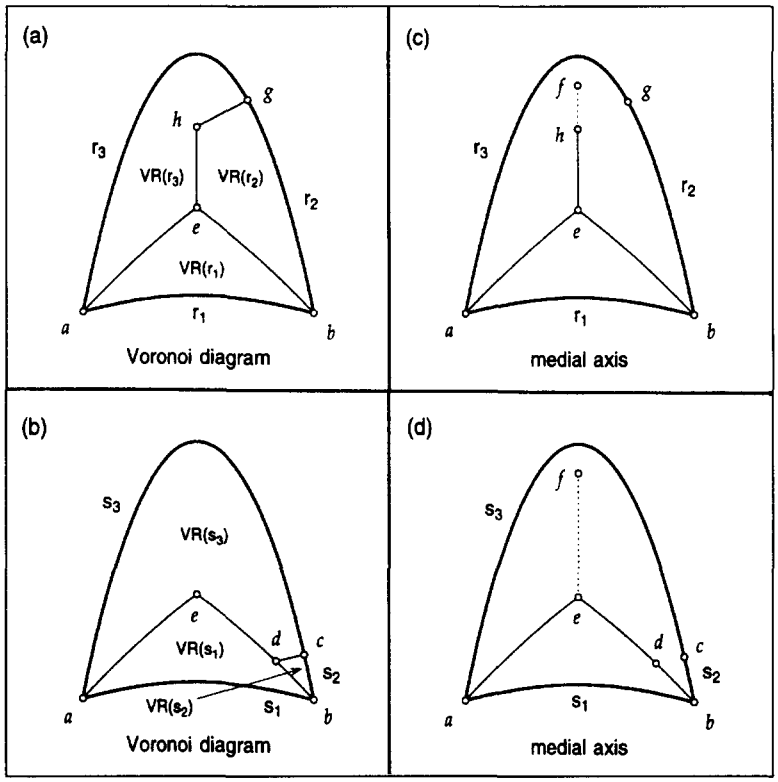

Fig. 9. In (a) and (b) the Voronoi diagram of the domain boundary S differs for the distinct segmentations, $S = r_1 \cup r_2 \cup r_3$ and $S = s_1 \cup s_2 \cup s_3$, of the boundary. However, the medial axes for these two segmentations, in (c) and (d), are seen to be identical (although their construction details differ).

precisely the edges that must be removed in step (i). We also noted that the medial axis edges, absent from the Voronoi diagram, that must be added in step (ii) are the interior self-bisectors (if any) of each individual boundary segment. These may be computed by the algorithm described in [19]. Once they are merged [13] with the Voronoi edges remaining from step (i), the complete medial axis is obtained.

To render the self-bisector computations tractable, a preprocessing step is invoked prior to commencement of the Voronoi diagram algorithm, in which certain segments of the boundary are subdivided into 'simpler' subsegments. A *simple* segment is defined [19] such that each point of its self-bisector has at most two interior footpoints on it – i.e., its interior self-bisector cannot bifurcate. In [19] it is shown that conics are always simple, while (polynomial) cubics can be split into at most three simple subsegments. Thus, in cases of practical interest, the preprocessing poses no computational difficulty. [14]

[13] Note that, in general, these self-bisectors 'connect' with the Voronoi edges remaining after step (i) in *critical* points (i.e., tangent discontinuities – see [18]) of the latter.

[14] Alt and Schwarzkopf [2] propose a more stringent preparatory subdivision, in which the resulting segments are guaranteed to have null interior self-bisectors, although they do not make a clear distinction between the Voronoi diagram

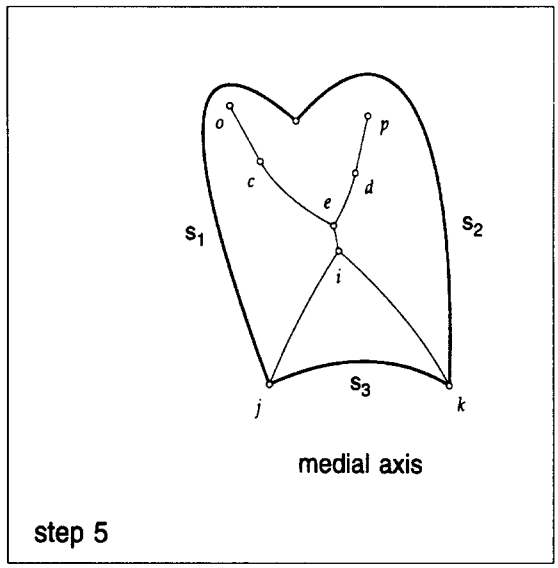

Fig. 10. Computing the medial axis from the Voronoi diagram in step 5. The Voronoi edges *bc* and *bd* in Fig. 7 have only one footpoint (at *b*) on the boundary, and are therefore removed. The interior self-bisectors of s_1 and s_2, namely the segments *co* and *dp*, are then added to obtain the complete medial axis (note that s_3 has no interior self-bisector within the boundary).

Because of the VD dependence on the boundary segmentation (see Section 7.3), it is necessary when treating boundaries with non-simple segments to decide *a priori* whether the Voronoi diagram or the medial axis is the ultimate goal. In the former case, no initial splitting into simple segments is invoked, and the computed VD is that for the original boundary segmentation. In the latter case, splitting into simple segments is required, and the intermediate VD produced in generating the MA is *not* that of the original segmentation.

8.1. *Worked example*

Finally, we complete the worked example of Section 5 by computing the medial axis of the domain from the interior Voronoi diagram of its boundary.

5. First, edges of the interior Voronoi diagram whose points have a *unique* footpoint on the boundary are deleted. Thus, the edges *bc* and *bd* in Fig. 7 are removed. Next, the interior self-bisector of each boundary segment is added to the remaining interior Voronoi edges. The edges *co* and *dp* are the interior self-bisectors of boundary segments s_1 and s_2 in Fig. 10, while segment s_3 has no interior self-bisector. These two operations yield the medial axis of the domain.

9. Closure

The Voronoi diagram/medial axis algorithm sketched above applies equally to the boundaries of both simply- and multiply-connected domains – since, during the merge process, no stipulation that

---

and medial axis (note also that the characterization of osculating circles given in [2] is incorrect).

the domain be simply-connected was necessary. The method is compatible with domains bounded by linear, conic, cubic, and higher-order polynomial or rational segments, and invokes point/curve and curve/curve bisector algorithms [16–19] developed previously, which guarantee exact capture of all rational bisector segments, and approximation of non-rational segments to a user-specified geometrical tolerance. The output is a set of polynomial or rational Bézier segments that represent the Voronoi diagram/medial axis edges exactly when possible, and otherwise approximate them rationally within the desired tolerance.

For brevity we have confined our present discussion to just a 'high-level' sketch of the algorithm, with a thorough treatment of the theoretical issues it entails. The companion paper [37] will include a more detailed description of the key implementation issues, together with more substantive computed examples of Voronoi diagrams and medial axes.

Acknowledgements

This work was supported by the National Science Foundation (CCR-9530741) and the Office of Naval Research (N00014-95-1-0767).

References

[1] N. Ahuja, A transform for multiscale image segmentation by integrated edge and region detection, IEEE Trans. Pattern Anal. Machine Intell. 18 (1996) 1211–1235.
[2] H. Alt, O. Schwarzkopf, The Voronoi diagram of curved objects, Proc. 11th ACM Comput. Geom. Symp. Vancouver, BC, 1995, pp. 89–97.
[3] F. Aurenhammer, Voronoi diagrams – survey of a fundamental geometric data structure, ACM Comput. Surveys 23 (1991) 345–405.
[4] H. Blum, A transformation for extracting new descriptors of shape, in: W. Wathen-Dunn (ed.), Models for the Perception of Speech and Visual Form, MIT Press, Cambridge, MA, 1967, pp. 362–380.
[5] H. Blum, R.N. Nagel, Shape description using weighted symmetric axis features, Pattern Recognition 10 (1978) 167–180.
[6] F.L. Bookstein, The line-skeleton, Comput. Graph. Image Process. 11 (1979) 123–137.
[7] J.W. Brandt, Convergence and continuity criteria for discrete approximations of the continuous planar skeleton, CVGIP: Image Understanding 59 (1994) 116–124.
[8] J.W. Brandt, V. R. Algazi, Continuous skeleton computation by Voronoi diagram, CVGIP: Image Understanding 55 (1992) 329–338.
[9] J.W. Brandt, A.K. Jain, V.R. Algazi, Medial axis representation and encoding of scanned documents, J. Visual Commun. Image Representation 2 (1991) 151–165.
[10] J.W. Bruce, P.J. Giblin, C.G. Gibson, Symmetry sets, Proc. Roy. Soc. Edinburgh Sect. A 101 (1985) 163–186.
[11] L. Calabi, W.E. Hartnett, Shape recognition, prairie fires, convex deficiencies, and skeletons, Amer. Math. Monthly 75 (1968) 335–342.
[12] H.I. Choi, S.W. Choi, H.P. Moon, Mathematical theory of medial axis transform, Pacific J. Math. 181 (1997) 57–88.
[13] H.I. Choi, S.W. Choi, H.P. Moon, N.S. Wee, New algorithm for medial axis transform of plane domain, Graph. Models Image Process. 59 (1997) 463–483.
[14] J.J. Chou, Numerical control milling machine toolpath generation for regions bounded by free form curves, PhD Thesis, University of Utah, (1989).
[15] J.J. Chou, Voronoi diagrams for planar shapes, IEEE Comput. Graph. Appl. 15 (3) (1995) 52–59.
[16] R.T. Farouki, J.K. Johnstone, The bisector of a point and a plane parametric curve, Comput. Aided Geom. Design 11 (1994) 117–151.

[17] R.T. Farouki, J.K. Johnstone, Computing point/curve and curve/curve bisectors, in: R.B. Fisher (ed.), Design and Application of Curves and Surfaces (The Mathematics of Surfaces V) Oxford University Press, Oxford, 1994, pp. 327–354.
[18] R.T. Farouki, R. Ramamurthy, Specified-precision computation of curve/curve bisectors, Internat. J. Comput. Geom. Appl. 8 (1998) 599–617.
[19] R.T. Farouki, R. Ramamurthy, Degenerate point/curve and curve/curve bisectors arising in medial axis computations for planar domains with curved boundaries, Comput. Aided Geom. Design 15 (1998) 615–635.
[20] D.S. Fritsch, S.M. Pizer, B.S. Morse, D.H. Eberly, A. Liu, The multiscale medial axis and its applications in image registration, Pattern Recognition Lett. 15 (1994) 445–452.
[21] P.J. Giblin, S.A. Brassett, Local symmetry of plane curves, Amer. Math. Monthly 92 (1985) 689–707.
[22] K.G.A. Gilhuijs, A. Tuow, M. Vanherk, R.E. Vijlbrief, Optimization of automatic portal image analysis, Med. Phys. 22 (1995) 1089–1099.
[23] L.M. Gross, Transfinite surface interpolation over Voronoi diagrams, PhD Thesis, Arizona State University (1995).
[24] H.N. Gursoy, Shape interrogation by medial axis transform for automated analysis, PhD Thesis, MIT (1989).
[25] H.N. Gursoy, N.M. Patrikalakis, An automatic coarse and fine surface mesh generation scheme based on the medial axis transform, I: algorithms, Engrg. Comput. 8 (1992) 121–137.
[26] M. Held, On the Computational Geometry of Pocket Machining, Springer, Berlin (1991).
[27] D.-S. Kim, I.-K. Hwang, B.-J. Park, Representing the Voronoi diagram of a simple polygon using rational quadratic Bézier curves, Comput. Aided Design 27 (1995) 605–614.
[28] R. Kunze, F.-E. Wolter, T. Rausch, Geodesic Voronoi diagrams on parametric surfaces, in: Proc. Computer Graphics Internat., CGI '97, IEEE Computer Society Press, Silver Spring, MD (1997) pp. 230–237.
[29] D.T. Lee, Medial axis transformation of a planar shape, IEEE Trans. Pattern Anal. Machine Intell. 4 (1982) 363–369.
[30] S.N. Meshkat, C.M. Sakkas, Voronoi diagram for multiply-connected polygonal domains II: Implementation and application, IBM J. Res. Develop. 31 (1987) 373–381.
[31] U. Montanari, Continuous skeletons from digitized images, J. Assoc. Comput. Mach. 16 (1969) 534–549.
[32] B.S. Morse, S.M. Pizer, A. Liu, Multiscale medial analysis of medical images, Image Vision Comput. 12 (1994) 327–338.
[33] A. Okabe, B. Boots, K. Sugihara, Spatial Tesselations: Concepts and Applications of Voronoi Diagrams, Wiley, New York (1992).
[34] H. Persson, NC machining of arbitrarily shaped pockets, Comput. Aided Design 10 (1978) 169–174.
[35] F.P. Preparata, The medial axis of a simple polygon, in: Proc. 6th Symp. on Mathematical Foundations of Computer Science (1977) pp. 443–450.
[36] F.P. Preparata, M.I. Shamos, Computational Geometry: An Introduction, 2nd ed., Springer, New York (1988).
[37] R. Ramamurthy, R.T. Farouki, Voronoi diagram and medial axis algorithm for planar domains with curved boundaries II. Detailed algorithm description (1999) to appear.
[38] T. Rausch, F.-E. Wolter, O. Sniehotta, Computation of medial curves on surfaces, in: T.N.T. Goodman, R.R. Martin (eds.), The Mathematics of Surfaces VII, Information Geometers (1997) pp. 43–68.
[39] T.W. Sederberg, S.R. Parry, Comparison of three curve intersection algorithms, Comput. Aided Design 18 (1986) 58–64.
[40] E.C. Sherbrooke, N.M. Patrikalakis, F.-E. Wolter, Differential and toplogical properties of medial axis transforms, Graph. Models Image Process. 58 (1996) 574–592.
[41] V. Srinivasan, L.R. Nackman, Voronoi diagram for multiply-connected polygonal domains I: Algorithm, IBM J. Res. Develop. 31 (1987) 361–372.
[42] V. Srinivasan, L.R. Nackman, J.-M. Tang, S.N. Meshkat, Automatic mesh generation using the symmetric axis transform of polygonal domains, IEEE Proc. 80 (1992) 1485–1501.
[43] T.K.H. Tam, C.G. Armstrong, 2D finite element mesh generation by medial axis subdivision, Adv. Engrg. Software 13 (1991) 313–324.
[44] G.M. Voronoi, Nouvelles applications des paramètres continus à la théorie des formes quadratiques, J. Reine Angew. Math. 134 (1908) 198–287.
[45] C.-K. Yap, An O(n log n) algorithm for the Voronoi diagram of a set of simple curve segments, Discrete Comput. Geom. 2 (1987) 365–393.